

Extracellular Biocoordinated Zinc Nanofibers Inhibit Malignant Characteristics of Cancer Cell

Qi Xin,[†] Haihui Zhang,^{†,‡} Qian Liu,[†] Zejian Dong,[†] Hongyu Xiang,^{*,‡} and Jian Ru Gong^{*,†}

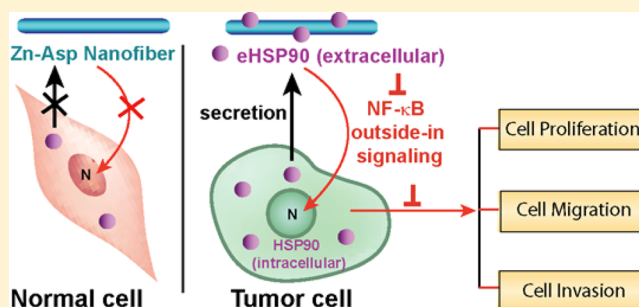
[†]CAS Key Laboratory of Nanosystem and Hierarchical Fabrication, National Center for Nanoscience and Technology, Beijing 100190, China

[‡]School of Life Sciences, Jilin University, Changchun 130012, China

S Supporting Information

ABSTRACT: Inhibition of the heat shock proteins (HSPs) has been considered to be one of the promising strategies for cancer treatment. However, developing highly effective HSP inhibitors remains a challenge. Recent studies on the evolutionarily distinct functions between intracellular and extracellular HSPs (eHSPs) trigger a new direction with eHSPs as chemotherapeutic targets. Herein, the first engineered eHSP nanoinhibitor with high effectiveness is reported. The zinc–aspartic acid nanofibers have specific binding ability to eHSP90, which induces a decrease in the level of the tumor marker–gelatinases, consequently resulting in downregulation of the tumor-promoting inflammation nuclear factor-kappa B signaling, and finally inhibiting cancer cell proliferation, migration, and invasion; while they are harmless to normal cells. Our findings highlight the potential for cancer treatment by altering the key determinants that shape its ability to adapt and evolve using novel nanomaterials.

KEYWORDS: Cancer inhibition, nanofiber, extracellular heat shock protein, NF-kappa B, nanobiomedicine



Instead of focusing on the tumor itself, cancer treatment would be achieved most effectively by altering the key determinants that shape its ability to adapt and evolve. Given that the increased expression of molecular chaperones can facilitate survival of tumor cells in their stressful microenvironment and allow tumor cells to tolerate mutation of signaling molecules,¹ pharmacological modulation of the molecular chaperone function is regarded as a promising chemotherapeutic.² Among the chaperones, the 90 kDa heat shock protein (HSP90) is unique because it is required for biogenesis of most proteins that have been linked to almost all hallmarks of cancer, one of the best choices in chaperone inhibition.^{3,4} Many inhibitors have been developed to target HSP90,^{5,6} but none of them has been approved so far for cancer treatment.⁷ The failure is mainly considered as ignorance of the evolutionarily distinct functions of intracellular and extracellular HSP90 (eHSP90) in cancer progression. Compared to the chaperone activity of intracellular HSP90, eHSP90 can act as an accessory protein to bind and activate cell surface receptors or secreted proteins, subsequently initiate outside-in signaling events and finally promote cancer progression.⁸ Hence, nondiscriminative targeting both intracellular and extracellular HSP90 makes the inhibitors inefficient.^{9–11} Furthermore, the membrane-permeable inhibitors of HSP90 have prohibitive side-effects because of the impairment of normal cellular functions.^{10,11} All these studies trigger a new direction for developing eHSP90 as a chemotherapeutic target.^{12–14}

With the development of nanoscience, there has been great progress in the field of nanomedicine for cancer treatment, especially for applications of nanomaterials.^{15,16} It is reported that nanomaterials can bind biological molecules with high capacity and affinity.^{17,18} In addition, the composition, size, and shape of the nanomaterial can be finely controlled.^{16,19–21}

Herein, we propose that zinc–aspartic acid (Zn-Asp) nanofibers (NFs) as the first nanoplatform can strongly interact with eHSP90 to inhibit malignant characteristics of cancer cell. It is based on three features of this material: (I) zinc ions are required for HSP90 activity.²² (II) Zinc ions and amino acids as essential elements and building units in human body have good biocompatibility.^{23,24} (III) The NFs with the average axial dimension several times bigger than the general size of human cells can be retained in the extracellular environment.²⁵ Our well-designed Zn-Asp NFs can specifically bind eHSP90 constitutively secreted from the cancer cell, which results in downregulation of the tumor-promoting inflammation nuclear factor-kappa B (NF-κB) outside-in signaling, and finally inhibits cancer cell proliferation, migration, and invasion; while they are harmless to the normal cell from which no eHSP90 is secreted (Scheme 1).

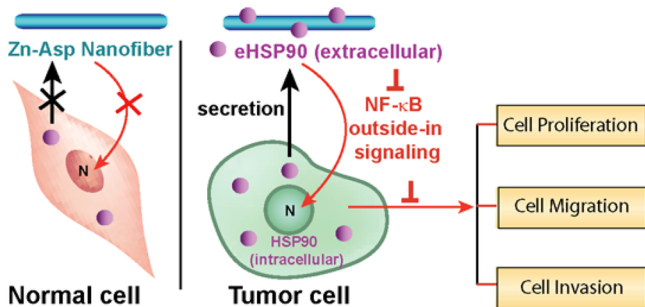
The D-/L-(Zn-Asp) NFs were synthesized through aqueous/organic interfacial polymerization of D-/L-aspartic acid with zinc

Received: May 17, 2015

Revised: September 17, 2015

Published: September 24, 2015

Scheme 1. Zn-Asp Nanofiber Can Specifically Bind eHSP90, Leading to Downregulation of the NF- κ B Outside-in Signaling, and Finally Inhibiting Cancer Cell Proliferation, Migration, and Invasion; while They Are Harmless to the Normal Cell from Which No eHSP90 Is Secreted^{4f}



^a“⊥” represents inhibition, and “N” is the nucleus of the cell.

ions under ambient conditions. Based on the coordination ability of carboxyl and amino groups from Asp to zinc metal ions, the sodium Asp in the ethanol and Zn(II) ions in the aqueous phase start to polymerize at the interface and grow oriented along the diffusion direction to form the Zn-Asp NFs.^{26,27} The NFs are highly uniform with sub-100 nm in diameter and over 30 μ m in length (Figure 1a and Figure S1 in

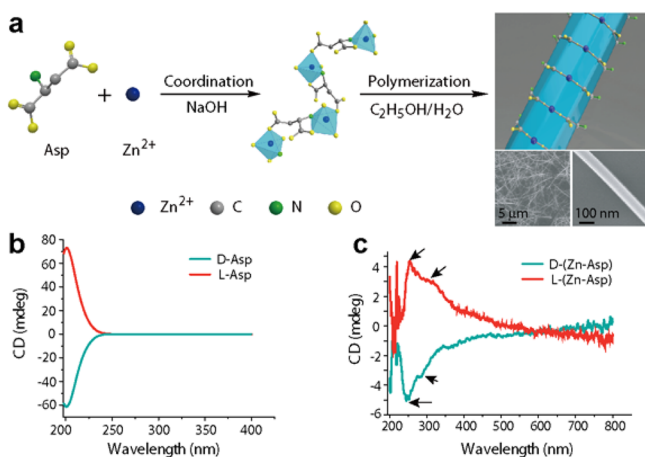


Figure 1. (a) Schematic diagram illustrates the coordinative polymerization of the Zn-Asp nanofiber. The large-scale and high-resolution scanning electron microscope images of the Zn-Asp nanofiber (bottom, right). CD spectra of (b) D- and L-Asp and (c) D- and L-(Zn-Asp) NFs.

Supporting Information). Compared with the pure D-/L-Asp that showed a circular dichroism (CD) peak at around 200 nm (Figure 1b), two additional CD (Figure 1c) and UV-vis (Figure S2) absorption peaks of the D-/L-(Zn-Asp) NFs at about 250 and 300 nm were attributed to the ligand (carboxyl and amino group)-to-metal charge-transfer transition of the coordinative polymer, indicating that the coordinative interaction of the chiral ligand Asp with zinc ions can induce novel chirality of the compound.²⁸ It is reported that the cellular response to nanomaterials is chirality-dependent,²⁹ so the possible different biochemical effects of D- and L-(Zn-Asp) NFs on cancer cell were also investigated in our experiment.

To evaluate the inhibitory capability of the Zn-Asp NFs on the viability in the cancer cell proliferation, the Cell Counting Kit-8 (CCK-8) assay was performed. A549 (human lung

carcinoma cell line) was chosen as a cancer cell model because it can overexpress and constitutively secrete HSP90. Considering that serum starvation can increase secretion of the tumor associated proteins, the cell viability was first determined under 1% fetal bovine serum (FBS) condition. After 24 h incubation with the D-/L-(Zn-Asp) NFs in a dose of 100 μ g mL⁻¹, the cell viability decreased by 27 and 25%, respectively (Figure 2a).

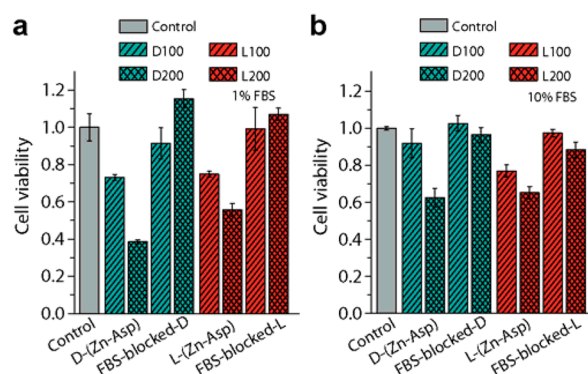


Figure 2. A549 cells were incubated with the D-/L-(Zn-Asp) NFs at the concentration of 100 (D-/L-100) and 200 (D-/L-200) μ g mL⁻¹ and the FBS-blocked NFs at the concentration of 100/200 μ g mL⁻¹ in the Dulbecco's modified Eagle's medium supplemented with (a) 1% and (b) 10% FBS, respectively. After 24 h, the cell viability was assayed by the CCK-8 assay. The results are means \pm standard error of the mean (S.E.M.) for biological replicates ($n = 5$).

When the concentration was increased to 200 μ g mL⁻¹, the D-/L-(Zn-Asp) NFs could cause 61 and 44% inhibition in the cell viability, respectively. Furthermore, a decrease in the inhibition of cell viability was found in the two control experiments (increasing the FBS concentration in the culture medium and blocking the binding sites of the NFs by FBS), indicating that the amount of the cancer-associated proteins bound on the NFs decreased after surplus FBS adsorbed. In contrast, the D-/L-(Zn-Asp) NFs have little inhibitory effect on the viability in the normal cell proliferation (human fetal lung fibroblast cells, MRC-5, Figure S3). The above results demonstrate that the Zn-Asp NFs effectively inhibit the tumor cell proliferation while harmless to normal cells, and the inhibitory effect is due to binding of the tumor-associated proteins on the NFs.

Next, a series of experiments were performed to identify the specific tumor-associated proteins in the extracellular environment that determine the above inhibitory effect of the Zn-Asp NFs on cancer cells. HSP90 was first verified as the protein that specifically bound on the NFs in the cell culture medium by sodium dodecyl sulfate polyacrylamide gel electrophoresis (SDS-PAGE) and matrix-assisted laser desorption/ionization time-of-flight mass spectrometry (Figure S4, Table S1). To further confirm this result, the binding between the NFs and the purified recombinant HSP90 protein at different concentrations was tested. The SDS-PAGE analysis showed that the proteins bound on the NFs increased with increasing concentration of HSP90 (Figure 3a), and the quantitative analysis of the Commassie Brilliant Blue (CBB) staining intensity of the protein band was summarized in Figure 3b with the D- and L-(Zn-Asp) NFs displaying a similar binding ability. Dominating amount and much stronger binding ability of HSP90 to the NFs compared to other HSPs in the affinity chromatography assay prove that HSP90 is the core protein of the multicomponent chaperone machinery (Figure S5). The

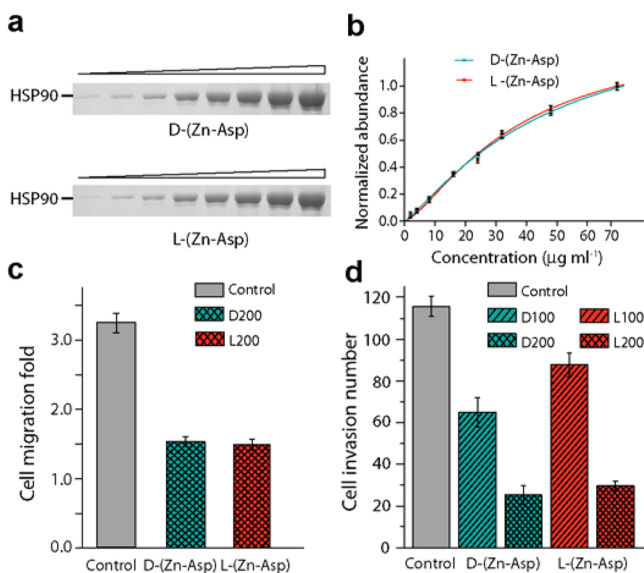


Figure 3. (a) Binding activity of the D-/L-(Zn-Asp) NFs to HSP90 was analyzed by SDS-PAGE and CBB staining. (b) Normalized protein abundance profile of the D-/L-(Zn-Asp). Relative values normalized to the maximum amount (set to 1) across concentration points for HSP90 are shown. (c) Cell migration of the untreated A549 cells and the A549 cells incubated with the D-/L-(Zn-Asp) NFs at the concentration of $200 \mu\text{g mL}^{-1}$ for 24 h were compared in the scratch-wound assay. (d) Cell invasion of the untreated A549 cells and the A549 cells incubated with the D-/L-(Zn-Asp) NFs at the concentrations of $100/200 \mu\text{g mL}^{-1}$ for 24 h were compared in the transwell assay. The results are means \pm SEM for biological replicates ($n = 5$).

binding of HSP90 to the NFs and subsequent decrease of the extracellular level of the tumor marker-gelatinases (Figure S6) are responsible for the inhibitory effect on the cancer cell proliferation.

HSP90 plays a critical role extracellularly in cancer progression, especially in promotion of cancer cell migration and invasion.³⁰ Since the Zn-Asp NFs might affect the activity of eHSP90, their influence on cancer cell migration and invasion was evaluated. Both D- and L-(Zn-Asp) NFs reduced the cell migration by nearly 54% after 24 h incubation at the concentration of $200 \mu\text{g mL}^{-1}$ in the scratch-wound assay (Figure 3c). The cell invasion was inhibited 43, 78, 22, and 74% (Figure 3d) compared with the control group, respectively, after incubating A549 cells with the D-/L-(Zn-Asp) NFs at different concentrations (100 and $200 \mu\text{g mL}^{-1}$) for 24 h in the transwell assay. These results indicate that the NFs can inhibit eHSP90 associated cell migration and invasion.

The secreted HSP90 can accelerate activation of NF- κ B signaling to promote cancer progression.³¹ In NF- κ B signaling, I κ B α protein is rapidly phosphorylated by I κ B kinases (IKK α , IKK β , and IKK γ), then the phosphorylated I κ B α (Ser32/S36) is ubiquitinated and degraded, which allows NF- κ B (p50/p52-p65 dimer) to enter the nucleus where it regulates the oncogene expression (Figure 4a).³² Consequently, the effect of the binding between eHSP90 and the Zn-Asp NFs on NF- κ B signaling was investigated at two different levels. At the gene level, the expression of NF- κ B-related genes was detected using the real-time polymerase chain reaction (real-time PCR). The data demonstrate that the incubation of NFs can induce downregulation of the gene expression levels of I κ B α , p50, and p52, and may downregulate p65 (Figure 4b). At the protein

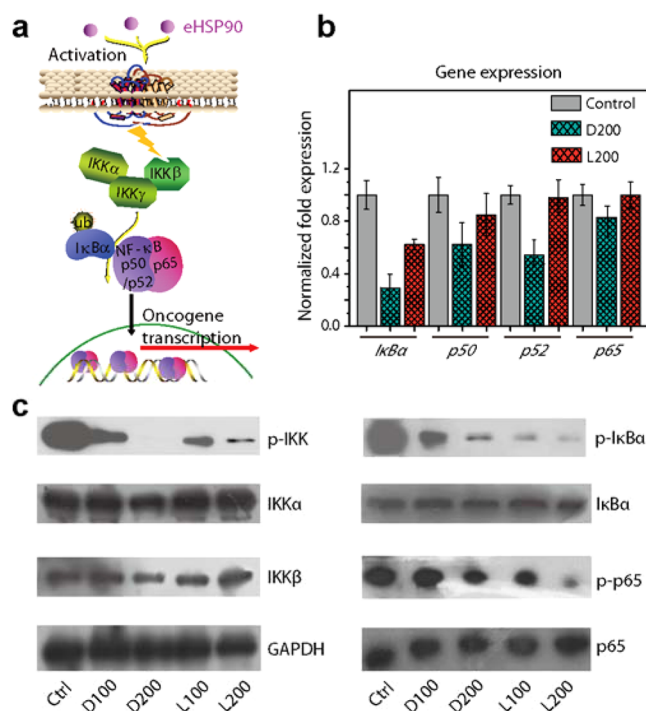


Figure 4. (a) Schematic diagram illustrates the NF- κ B signaling pathway. (b) A549 cells were incubated with the D-/L-(Zn-Asp) NFs at the concentration of $200 \mu\text{g mL}^{-1}$ for 24 h, respectively. The mRNA expression levels of the NF- κ B related genes were analyzed by real-time PCR. (c) A549 cells were incubated with the D-/L-(Zn-Asp) NFs at the concentration of $100/200 \mu\text{g mL}^{-1}$ for 24 h. The total and phosphorylated levels of the NF- κ B related proteins (IKK α , IKK β , I κ B α , and p65) were tested by Western blot. The constitutively expressed GAPDH served as a loading control.

level, the site-specific phosphorylation level of the NF- κ B signaling components was determined by Western blot. The data showed that the protein levels of phospho-IKK α/β (Ser176/180), phospho-I κ B α (Ser32), and phospho-p65 (Ser536) significantly decreased after incubation with the NFs, while the total levels of IKK α , IKK β , I κ B α , and p65 did not change (Figure 4c). Taken together, the decrease in the mRNA and phosphorylation levels of the NF- κ B components display that incubation of the NFs can downregulate NF- κ B signaling, which leads to inhibition of cancer cell migration and invasion. Although both D- and L-(Zn-Asp) NFs can decrease the mRNA and phosphorylation level of NF- κ B, the magnitude of the decrease varies in some extent.

NF- κ B signaling can regulate autophagic response, which might lead to cancer suppression,³³ and the data from Western blot and biological transmission electron microscope tests revealed that both D- and L-(Zn-Asp) NFs could induce an autophagic response (Figures S7 and S8). In addition, the autophagic vacuoles contained some membrane-like structure instead of the long fibrous morphology of the Zn-Asp NFs (Figure S7c). Meanwhile, the result of the intracellular zinc ions assay demonstrates that the NFs perform their inhibitory effect on cancer cells in extracellular environment without entering cells (Figure S9). Otherwise, only trace amount of zinc ions released from the Zn-Asp NFs into the PBS was detected (Figure S10), indicating that the NFs could basically maintain the structural stability during the period of experiment.

Our results show that the D-/L-(Zn-Asp) NFs retained in the extracellular environment can specifically bind eHSP90, which

induces decrease in the level of gelatinases, resulting in downregulation of NF- κ B signaling and formation of autophagy, finally inhibiting cancer cell proliferation, migration, and invasion. The binding between the NFs and eHSP90, which contributes to the inhibitory effect, is mainly determined by the amount of zinc ions on the NFs. Furthermore, the amino acid moiety of the NFs could form hydrogen bond with the eHSP90, which might enhance the binding interaction,³⁴ and the intensity of the hydrogen bonds between chiral NFs and eHSP90 can be different considering the different spatial arrangements of the functional groups (the uncoordinated carboxyl and amine group of chiral Asp) on the surface of the two kinds of NFs.³⁵ Therefore, the binding between D-/L-(Zn-Asp) NFs and eHSP90 are not exactly the same, resulting in a slight difference in their inhibitory ability toward cancer cells proliferation, invasion, and NF- κ B signaling. In addition, it has been reported that NFs can be used in vivo for cancer therapy by implantation or local injection,^{36,37} and inhibition of eHSP90 has revealed antimigratory activity in melanoma and breast cancer.³⁸ The biodegradation result (Figure S11) demonstrates that the NFs can partly degrade after incubation for a long time, which might induce a zinc(II)-related inflammation response. Therefore, further improvement of the stability of the NFs by optimizing the composition, morphology, size, etc., will benefit the future clinical application. This approach opens up great opportunities for developing novel inhibitors for cancer treatment.

■ ASSOCIATED CONTENT

Supporting Information

The Supporting Information is available free of charge on the ACS Publications website at DOI: 10.1021/acs.nanolett.5b01926.

Experimental section; additional results and discussion; Figures S1–S11 (PDF)

■ AUTHOR INFORMATION

Corresponding Authors

*E-mail: gongjr@nanoctr.cn (J.R.G).

*E-mail: hyxiang@jlu.edu.cn (H.X).

Author Contributions

Q.X. and H.Z. contributed equally to this work.

Notes

The authors declare no competing financial interest.

■ ACKNOWLEDGMENTS

The authors gratefully acknowledge the financial support from National Natural Science Foundation of China (21422303, 21573049), Beijing Natural Science Foundation (2142036), National Basic Research Program of China (2011CB933401), the Knowledge Innovation Program of the Chinese Academy of Sciences, and Youth Innovation Promotion Association CAS.

■ REFERENCES

- (1) Whitesell, L.; Lindquist, S. L. *Nat. Rev. Cancer* **2005**, *5*, 761–772.
- (2) Taldone, T.; Ochiana, S. O.; Patel, P. D.; Chiosis, G. *Trends Pharmacol. Sci.* **2014**, *5*, 592–603.
- (3) Hanahan, D.; Weinberg, R. A. *Cell* **2011**, *144*, 646–674.
- (4) Neckers, L.; Workman, P. *Clin. Cancer Res.* **2012**, *18*, 64–76.
- (5) Trepel, J.; Mollapour, M.; Giaccone, G.; Neckers, L. *Nat. Rev. Cancer* **2010**, *10*, 537–549.
- (6) Wang, J.; et al. *Cancer Lett.* **2015**, *362*, 83–96.

- (7) Garcia-Carbonero, R.; Carnero, A.; Paz-Ares, L. *Lancet Oncol.* **2013**, *14*, 358–369.
- (8) Hance, M. W.; Nolan, K. D.; Isaacs, J. S. *Cancers* **2014**, *6*, 1065–1097.
- (9) Bhat, R.; Tummalapalli, S. R.; Rotella, D. P. *J. Med. Chem.* **2014**, *57*, 8718–8728.
- (10) Jhaveri, K.; et al. *Expert Opin. Invest. Drugs* **2014**, *23*, 611–628.
- (11) Sidera, K.; Patsavoudi, E. *Recent Pat. Anticancer Drug Discovery* **2014**, *9*, 1–20.
- (12) Tsutsumi, S.; Scroggins, B.; Koqa, F.; Lee, M. J.; Trepel, J.; Felts, S.; Carreras, C.; Nechers, L. *Oncogene* **2008**, *27*, 2478–2487.
- (13) Stellas, D.; Hamidieh, A.; Patsavoudi, E. *BMC Cell Biol.* **2010**, *11*, 51.
- (14) Li, W.; Tsen, F.; Sahu, D.; Bhatia, A.; Chen, M.; Multhoff, G.; Woodley, D. T. *Int. Rev. Cell Mol. Biol.* **2013**, *303*, 203–235.
- (15) Thakor, A. S.; Gambhir, S. S. *Ca-Cancer J. Clin.* **2013**, *63*, 395–418.
- (16) Hu, B.; Shi, W.; Wu, Y. L.; Leow, W. R.; Cai, P.; Li, S.; Chen, X. *Adv. Mater.* **2014**, *26*, 5786–5793.
- (17) Monopoli, M. P.; Aberg, C.; Salvati, A.; Dawson, K. A. *Nat. Nanotechnol.* **2012**, *207*, 779–786.
- (18) Lynch, I.; Dawson, K. A. *Nano Today* **2008**, *3*, 40–47.
- (19) Liu, Q.; Guo, B.; Rao, Z.; Zhang, B.; Gong, J. R. *Nano Lett.* **2013**, *13*, 2436–2441.
- (20) Chen, E.; Guo, B.; Zhang, B.; Gan, L. H.; Gong, J. R. *J. Nanosci. Nanotechnol.* **2011**, *11*, 7682–7686.
- (21) Gong, J. R. *Small* **2010**, *6*, 967–973.
- (22) Joseph, K.; Tholanikunnel, B. G.; Kaplan, A. P. *Proc. Natl. Acad. Sci. U. S. A.* **2002**, *99*, 896–900.
- (23) Tapiero, H.; Tew, K. D. *Biomed. Pharmacother.* **2003**, *57*, 399–411.
- (24) Millward, D. J.; Layman, D. K.; Tome, D.; Schaafsma, G. *Am. J. Clin. Nutr.* **2008**, *87*, 1576–1581.
- (25) Yoo, H. S.; Kim, T. G.; Park, T. G. *Adv. Drug Delivery Rev.* **2009**, *61*, 1033–1042.
- (26) Imaz, I.; Rubio-Martinez, M.; Saletta, W. J.; Amabilino, D. B.; Maspocho, D. *J. Am. Chem. Soc.* **2009**, *131*, 18222–18223.
- (27) Gould, J. A.; Jones, J. T.; Bacsa, J.; Khimiyak, Y. Z.; Rosseinsky, M. J. *Chem. Commun.* **2010**, *46*, 2793–2795.
- (28) Li, C.; Deng, K.; Tang, Z.; Jiang, L. *J. Am. Chem. Soc.* **2010**, *132*, 8202–8209.
- (29) Li, Y.; Zhou, Y.; Wang, H. Y.; Perrett, S.; Zhao, Y.; Tang, Z.; Nie, G. *Angew. Chem., Int. Ed.* **2011**, *50*, 5860–5864.
- (30) Eustace, B. K.; et al. *Nat. Cell Biol.* **2004**, *6*, 507–514.
- (31) Chen, J. S.; Hsu, Y. M.; Chen, C. C.; Chen, L. L.; Lee, C. C.; Huang, T. S. *J. Biol. Chem.* **2010**, *285*, 25458–25466.
- (32) Hoffmann, A.; Levchenko, A.; Scott, M. L.; Baltimore, D. *Science* **2002**, *298*, 1241–1245.
- (33) Salminen, A.; Hyttinen, J. M.; Kauppinen, A.; Kaarniranta, K. *Int. J. Cell Biol.* **2012**, *2012*, 849541.
- (34) Kubinyi, H. *Pharmacokinetic Optimization in Drug Research: Biological, Physicochemical, and Computational Strategies*; John Wiley & Sons: Switzerland, 2007.
- (35) Chang, B.; Zhang, M.; Qing, G.; Sun, T. *Small* **2015**, *11*, 1097–1112.
- (36) Hsieh, P. C.; Davis, M. E.; Gannon, J.; Mac Gillivray, C.; Lee, R. T. *J. Clin. Invest.* **2006**, *116*, 237–348.
- (37) Yang, G.; Wang, J.; Wang, Y.; Li, L.; Guo, X.; Zhou, S. *ACS Nano* **2015**, *9*, 1161–1174.
- (38) Tsutsumi, S.; Beebe, K.; Neckers, L. *Future Oncol.* **2009**, *5*, 679–688.